HNUE JOURNAL OF SCIENCE DOI: 10.18173/2354-1059.2021-0048
Natural Sciences 2021, Volume 66, Issue 3, pp. 69-80
This paper is available online at http://stdb.hnue.edu.vn

THERMODYNAMIC PROPERTY OF ALLOY FCC-AuCuLi AT ZERO PRESSURE

Nguyen Quang Hoc[1] and Nguyen Duc Hien[2]
[1]*Faculty of Physics, Hanoi National University of Education,*
[2]*Mac Dinh Chi High School, Chu Pah, Gia Lai*

Abstract. We briefly present the thermodynamic theory of FCC ternary substitutional and interstitial alloy at zero pressure derived by the statistical moment method and apply this theory to alloy AuCuLi. The thermodynamic properties of Au, AuCu and AuLi are specific cases for that of AuCuLi. We compare the thermodynamic properties of alloys AuCuSi and AuCuLi. Our calculated results of thermodynamic quantities for AuCuLi predict and orient experimental results in the future.

Keywords: ternary substitutional and interstitial alloy, statistical moment method, alloy AuCuLi, thermodynamic property.

1. Introduction

The thermodynamic and elastic properties of interstitial alloys attract the interest of many researchers [1-5].

Gold (Au) and its alloys have many important applications. Au is a metal with high ductility and structural stability under extreme pressure and temperature conditions [6, 7]. Au has a face-centered cubic (FCC) structure, which is stable at pressure P = 600 GPa and ambient temperature [8]. Au is widely used in industries such as photocatalysis for drugs [9]. At 0.1 MPa, Au has an FCC structure with the lattice constant $a = 4.0785$ Å at 25^{o}C and the melting point at 1064 ^{o}C [10]. Gold in a solid state was studied by the equation of state [11, 12] and by calculations [13-17]. The melting curve of alloy AuCu was studied in [18]. Elastic deformation of alloys AuLi and AuCuLi was considered in [19].

In the pressent paper, we briefly show our thermodynamics of FCC ternary alloy built by the statistical moment method (SMM) [19-27] and apply it to alloy AuCuLi. In our previous papers [28-31], we studied the thermodynamic properties of alloys AuSi and AuCuSi. Here we substitute the interstitial atom Si by Li in order to show the role of the size of the interstitial atom and the interaction between this atom and the main metal atom.

Received August 18, 2021. Revised October 21, 2021. Accepted October 28, 2021.
Contact: Nguyen Quang Hoc, e-mail address: hocnq@hnue.edu.vn

2. Content

2.1. Thermodynamic theory of FCC ternary substitutional and interstitial alloy

The FCC substitutional and interstitial alloy ABC (the substitution alloy AB with C interstitial atom, where the interstitial atom C stays in body center and the substitutional atom B stays in face center of cubic unit cell) has N atoms (N_A main atoms A, N_B substitutional atoms B and N_C interstitial atoms C). The concentrations of alloy components are $c_A = \frac{N_A}{N}, c_B = \frac{N_B}{N}$ and $c_C = \frac{N_C}{N}$ satisfy the condition $c_C << c_B << c_A$. The free energy of alloy ABC has the form [19, 20, 26, 27].

$$\psi_{ABC} = \psi_{AC} + c_B\left(\psi_B - \psi_A\right) + TS_c^{AC} - TS_c^{ABC},$$

$$\psi_{AC} = \left(1-15c_C\right)\psi_A + c_C\psi_C + 6c_C\psi_{A_1} + 8c_C\psi_{A_2} - TS_c^{AC},$$

$$\psi_X = U_{0X} + \psi_{0X} + 3N\left\{\frac{\theta^2}{k_X^2}\left[\gamma_{2X}Y_X^2 - \frac{2\gamma_{1X}}{3}\left(1+\frac{1}{2}Y_X\right)\right] + \right.$$

$$\left. + \frac{2\theta^3}{k_X^4}\left[\frac{4}{3}\gamma_{2X}^2 Y_X\left(1+\frac{1}{2}Y_X\right) - 2\left(\gamma_{1X}^2 + \gamma_{1X}\gamma_{2X}\right)\left(1+\frac{1}{2}Y_X\right)\left(1+Y_X\right)\right]\right\},$$

$$\psi_{0X} = 3N\theta\left[x_X + \ln\left(1-e^{-x_X}\right)\right], X = A, B, C, A_1, A_2, Y_X \equiv x_X \coth x_X, x_X = \frac{\hbar\omega_X}{2\theta} = \frac{\hbar\omega_X}{2k_{Bo}T}\sqrt{\frac{k_X}{m_X}}, \quad (1)$$

where $\psi_{AC}, \psi_A, \psi_C, \psi_{A_1}, \psi_{A_2}$ respectively are the free energies of interstitial alloy AC, atom A in pure metal A, atom C in alloy ABC, atom A_1 (atom A in face centers of the cubic unit cell) and atom A_2 (atom A in peaks of the cubic unit cell), S_c^{AC}, S_c^{ABC} respectively are the configuration entropies of alloy AC and alloy ABC, $k_X, \gamma_{1X}, \gamma_{2X}, \gamma_X = 4\left(\gamma_{1X} + \gamma_{2X}\right)$ are the alloy's parameters [19, 26], m_X is the mass of atom X, $U_{0X} = \frac{N}{2}u_{0X}, u_{0X}$ is the cohesive energy of atom X, T is the absolute temperature and k_{Bo} is the Boltzmann constant.

The mean nearest neighbor distances between two atoms in the alloy ABC at temperature T is given by [19, 20, 27].

$$a_{ABC} = c_{AC}a_{AC}\frac{B_{TAC}}{\overline{B_T}} + c_B a_B \frac{B_{TB}}{\overline{B_T}}, \overline{B_T} = c_{AC}B_{TAC} + c_B B_{TB}, c_{AC} = c_A + c_C, a_{AC} = \overline{r_{1A}}(0,T),$$

$$B_{TM} = \frac{1}{\chi_{TM}}, \chi_{TM} = \frac{3\left(\frac{a_M}{a_{0M}}\right)^3}{\frac{\sqrt{2}}{a_M}\frac{1}{3N_M}\left(\frac{\partial^2\psi_M}{\partial a_M^2}\right)_T}, M = AC, B,$$

$$\left(\frac{\partial^2\psi_{AC}}{\partial a_{AC}^2}\right)_T=\left[\frac{\partial^2\psi_{AC}}{\partial\overline{r_{1A}^{-2}}(0,T)}\right]_T\approx\sum_X c_X\left(\frac{\partial^2\psi_X}{\partial a_x^2}\right)_T\quad X=A,C,A_1,A_2,c_A=1-15c_C,c_{A_1}=6c_C,c_{A_2}=8c_C,$$

$$\left(\frac{\partial^2\psi_X}{\partial a_X^2}\right)_T=\left(\frac{\partial^2\psi_A}{\partial r_{1X}^2(0,T)}\right)_T,\frac{1}{3N}\left(\frac{\partial^2\Psi_X}{\partial a_X^2}\right)_T=\frac{1}{6}\frac{\partial^2 u_{0X}}{\partial a_X^2}+\frac{\hbar\omega_X}{4k_X}\left[\frac{\partial^2 k_X}{\partial a_X^2}-\frac{1}{2k_X}\left(\frac{\partial k_X}{\partial a_X}\right)^2\right]. \qquad (2)$$

The isothermal compressibility χ_{TABC}, the elastic modulus B_{TABC}, the thermal expansion coefficient α_{TABC}, the heat capacity at constant volume C_{VABC} and the heat capacity at a constant pressure C_{PABC} of the alloy ABC has the form [20, 27].

$$\chi_{TABC}=\frac{3\left(\frac{a_{ABC}}{a_{0ABC}}\right)^3}{\frac{\sqrt{2}}{a_{ABC}}\frac{1}{3N}\left(\frac{\partial^2\psi_{ABC}}{\partial a_{ABC}^2}\right)_T},\quad B_{TABC}=\frac{1}{\chi_{TABC}},$$

$$\left(\frac{\partial^2\psi_{ABC}}{\partial a_{ABC}^2}\right)_T\approx\left(\frac{\partial^2\psi_{AC}}{\partial a_A^2}\right)_T+c_B\left[\left(\frac{\partial^2\psi_B}{\partial a_B^2}\right)_T-\left(\frac{\partial^2\psi_A}{\partial a_A^2}\right)_T\right]. \qquad (3)$$

$$\alpha_{TABC}=\frac{k_{Bo}}{\alpha_{0ABC}}\frac{da_{ABC}}{d\theta}=-\frac{k_{Bo}\chi_{TABC}}{3}\left(\frac{a_{0ABC}}{a_{ABC}}\right)^2\frac{a_{ABC}}{3v_{ABC}}\frac{\partial^2\psi_{ABC}}{\partial\theta\partial a_{ABC}},$$

$$\frac{\partial^2\psi_{ABC}}{\partial\theta\partial a_{ABC}}\approx\frac{\partial^2\psi_{AC}}{\partial\theta\partial a_{AC}}+c_B\left(\frac{\partial^2\psi_B}{\partial\theta\partial a_B}-\frac{\partial^2\psi_A}{\partial\theta\partial a_A}\right),\frac{\partial^2\psi_{AC}}{\partial\theta\partial a_{AC}}\approx\sum_X c_X\frac{\partial^2\psi_X}{\partial\theta\partial a_X},$$

$$\frac{\partial^2\psi_X}{\partial\theta\partial a_X}=\frac{3Z_X^2}{2k_X}\frac{\partial k_X}{\partial a_X}+\frac{6\theta^2}{k_X^2}\left[\frac{\gamma_{1X}}{3k_X}\frac{\partial k_X}{\partial a_X}\left(2+Y_XZ_X^2\right)-\right.$$

$$\left.-\frac{1}{6}\frac{\partial\gamma_{1X}}{\partial a_X}\left(4+Y_X+Z_X^2\right)-\left(\frac{2\gamma_{2X}}{k_X}\frac{\partial k_X}{\partial a_X}-\frac{\partial\gamma_{2X}}{\partial a_X}\right)Y_XZ_X^2\right],Z_X\equiv\frac{x_X}{\sinh x_X}. \qquad (4)$$

$$C_{VABC}\approx C_{VAC}+c_B\left(C_{VB}-C_{VA}\right),C_{VAC}=\sum_X c_XC_{VX},$$

$$C_{VX}=3Nk_{Bo}\left\{Z_X^2+\frac{2\theta}{k_X^2}\left[\left(2\gamma_2+\frac{\gamma_{1X}}{3}\right)Y_XZ_X^2+\frac{2\gamma_{1X}}{3}-\gamma_{2X}\left(Z_X^4+2Y_X^2Z_X^2\right)\right]\right\} \qquad (5)$$

$$C_{PABC}=C_{VABC}+\frac{9TV_{ABC}\alpha_{TABC}^2}{\chi_{TABC}}. \qquad (6)$$

2.2. Numerical results for alloy AuCuLi

For alloy AuCuLi, we use the Mie-Lennard-Jones potential

$$\varphi(r) = \frac{D}{n-m}\left[m\left(\frac{r_0}{r}\right)^n - n\left(\frac{r_0}{r}\right)^m \right], \tag{7}$$

where potential parameters for interactions Au-Au, Cu-Cu and Li-Li are given in Table 1. Interactions Au-Cu and Au-Li are approximately determined by

$$\varphi_{\text{Au-Cu}} \approx \frac{1}{2}\left(\varphi_{\text{Au-Au}} + \varphi_{\text{Cu-Cu}}\right), \varphi_{\text{Au-Li}} \approx \frac{1}{2}\left(\varphi_{\text{Au-Au}} + \varphi_{\text{Li-Li}}\right). \tag{8}$$

Table 1. The parameters m, n, D, r_0 ***of materials Au, Cu and Li [32]***

Material	***m***	***n***	$D\left(10^{-16}\text{erg}\right)$	$r_0\left(10^{-10}\text{m}\right)$
Au	5.5	10.5	6462.54	2.8751
Cu	5.5	11	4693.518	2.5487
Li	1.66	3.39	6800.502	3.0077

Our numerical results are described by figures from Figure 1 to Figure 12 and tables from Table 2 to Table 9. When the concentration $c_{\text{Li}} \to 0$ and the concentration $c_{\text{Cu}} \to 0,$ we obtain thermodynamic quantities of Au. Our calculated results in Table 2 and Table 3 are in good agreement with experiments [33].

Table 2. Dependence of thermal expansion coefficient $\alpha_T\left(10^{-5}\text{K}^{-1}\right)$ ***on temperature T for Au from SMM and EXPT [33]***

***T*(K)**	**100**	**200**	**300**	**500**	**700**	**1000**
α_T -SMM	1.19	1.37	1.44	1.55	1.66	1.91
α_T -EXPT	1.15	1.34	1.41	1.50	1.59	1.95
$\delta_{SMM-EXPT[25]}(\%)$	3.5	2.2	2.1	3.3	4.4	2.1

Table 3. Dependence of heat capacity at constant pressure $C_P\left(\text{J/mol.K}\right)$ ***on temperature T for Au from SMM and EXPT [33]***

***T*(K)**	**100**	**200**	**300**	**500**	**700**
C_P -SMM	21.7695	24.9163	25.9581	27.3465	28.6754
C_P -EXPT	21.4364	24.3253	25.1208	25.9581	26.7955
$\delta_{SMM-EXPT[25]}(\%)$	1.6	2.4	3.3	5.3	7.0

For AuCuSi at the same temperature and concentration of substitutional atoms Cu when the concentration of interstitial atoms Li increases, the mean nearest neighbor *a*, the heat capacity at constant pressure C_P increases và the thermal expansion coefficient α_T decreases. For example for AuCuLi at T = 1000 K and $c_{\mathrm{Cu}} = 6\%$ when c_{Li} increases from 0 to 5%, *a* increases from 2.8516 to 3.6067.10^{-10} m (see Table 4) (increases 26.5%), C_P increases from 31.081 to 47.6776 J/ mol.K (see Table 8) (increases 53.4%) and α_T decreases very strongly from 2.6015×10^{-5} to 0.2638×10^{-5} K^{-1} (see Table 6) (decreases 886%). For alloy AuCuLi at the same concentration of substitutional atoms Cu and concentration of interstitial atoms Li when the temperature increases, all quantities increase. For example for AuCuLi at $c_{\mathrm{Cu}} = 6\%$, and $c_{\mathrm{Li}} = 5\%$ when T increases from 50 to 1000 K, *a* increases from 2.9162 to 3.6067.10^{-10} m (see Table 4) (increases 23.7%), α_T increases from 0.199×10^{-5} to 0.2638×10^{-5} K^{-1} (see Table 6) (increases 32.6%) and C_P increases strongly from 14.7759 to 47.6776 J/mol.K (see Table 8) (increases 222,7%). For AuCuLi at the same temperature and concentration of interstitial atoms Li when the concentration of substitutional atoms Cu increases, α_T increases and *a*, C_P decrease. For example for AuCuLi at 1000K and $c_{\mathrm{Li}} = 0.6\%$ when c_{Cu} increases from 0 to 6%, *a* decreases slightly from 2.9743 to 2.9521.10^{-10} m (see Table 5) (decreases 0.75%) α_T increases slightly from 1.0819×10^{-6} to 1.1001×10^{-6} K^{-1} (see Table 7) (increases 1.7%) and C_P decreases slightly from 32.3474 to 31.8253 J/mol.K (see Table 9) (decreases 1.64%). The small change of thermodynamic quantities with a concentration of substitutional atoms are explained by the small difference of atom size between metals Au and Cu. At zero concentration of substitutional atoms Cu and zero concentration of interstitial atoms Li, the thermodynamic quantities of AuCuLi become the thermodynamic quantities of Au in [27]. The change of thermodynamic quantities with temperature for AuCuLi is similar to that for AuLi [26]. The change of thermodynamic quantities with temperature and concentration of substitutional atoms Cu for AuCuLi is similar to that for AuCu [25].

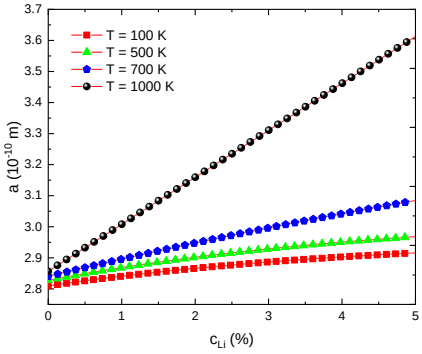

Figure 1. $a\left(c_{\mathrm{Li}},T\right)$ ***for AuCuLi at*** $c_{\mathrm{Cu}} = 6\%$

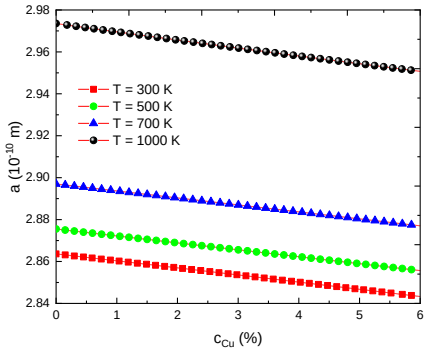

Figure 2. $a\left(c_{\mathrm{Cu}},T\right)$ ***for AuCuLi at*** $c_{\mathrm{Li}} = 0,6\%$

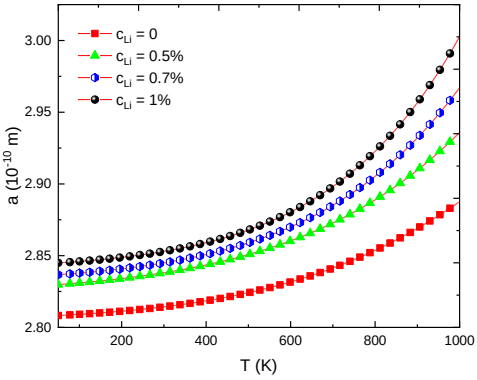

Figure 3. a(T, c_{Li}) for AuCuLi at $c_{\mathrm{Cu}} = 6\%$

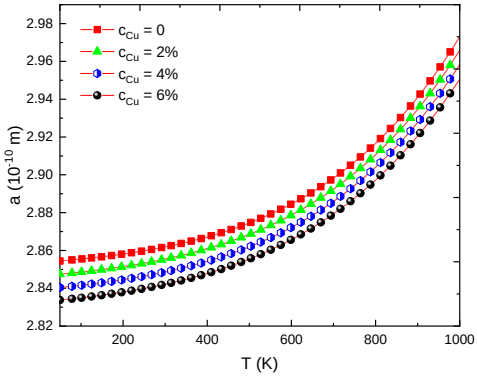

Figure 4. a(T, c_{Cu}) for AuCuLi at $c_{\mathrm{Li}} = 0,6\%$

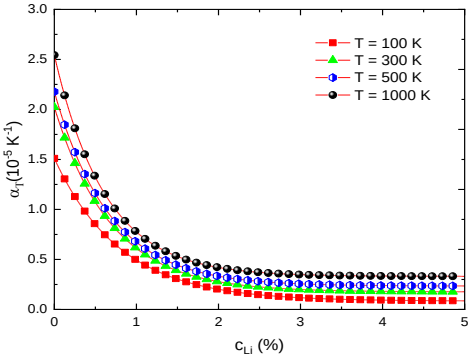

Figure 5. $\alpha_T\left(c_{\mathrm{Li}}, T\right)$ for AuCuLi at $c_{\mathrm{Cu}} = 6\%$

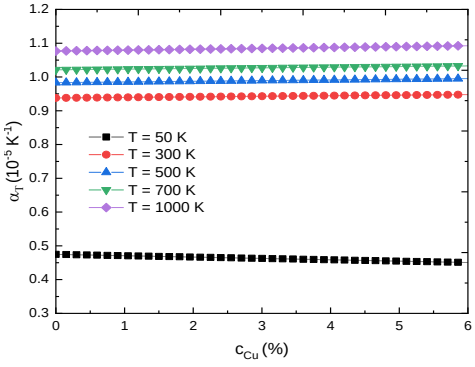

Figure 6. $\alpha_T\left(c_{\mathrm{Cu}}, T\right)$ for AuCuLi at $c_{\mathrm{Li}} = 0,6\%$

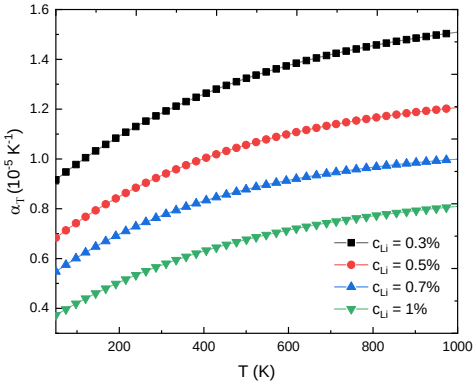

Figure 7. $\alpha_T\left(T, c_{\mathrm{Li}}\right)$ for AuCuLi at $c_{\mathrm{Cu}} = 6\%$

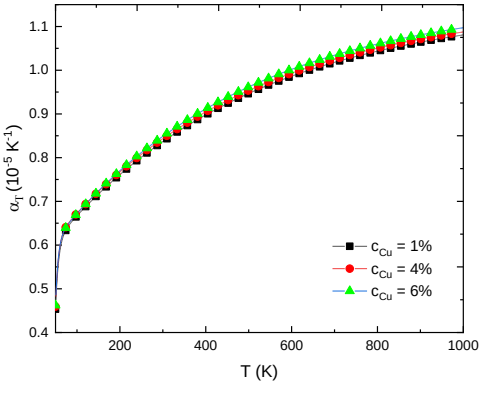

Figure 8. $\alpha_T\left(T, c_{\mathrm{Cu}}\right)$ for AuCuLi at $c_{\mathrm{Li}} = 0,6\%$

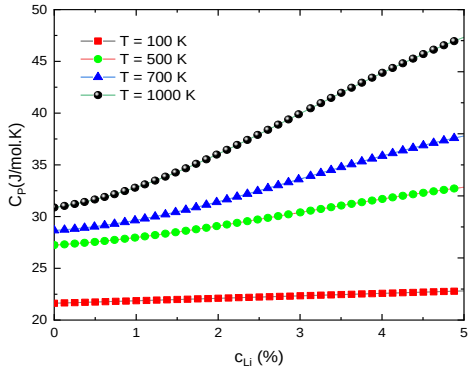

Figure 9. $C_P\left(c_{\mathrm{Li}},T\right)$ ***for AuCuLi at*** $c_{\mathrm{Cu}}=6\%$

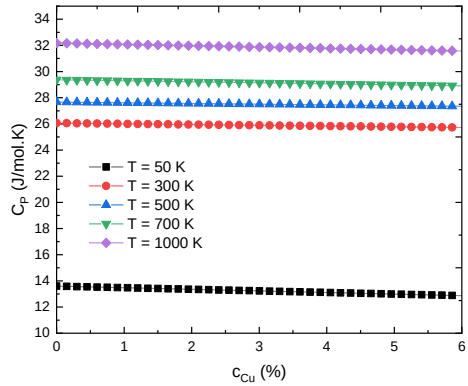

Figure 10. $C_P\left(c_{\mathrm{Cu}},T\right)$ ***for AuCuLi at*** $c_{\mathrm{Li}}=0,6\%$

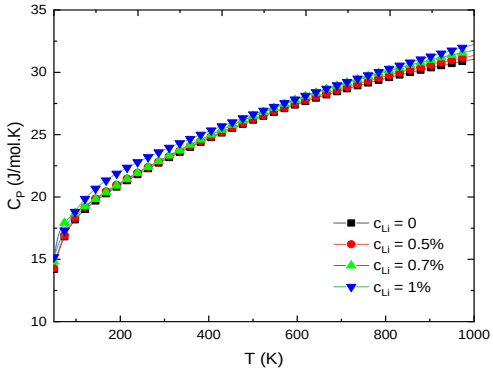

Figure 11. $C_P\left(T,c_{\mathrm{Li}}\right)$ ***for AuCuLi at*** $c_{\mathrm{Cu}}=6\%$

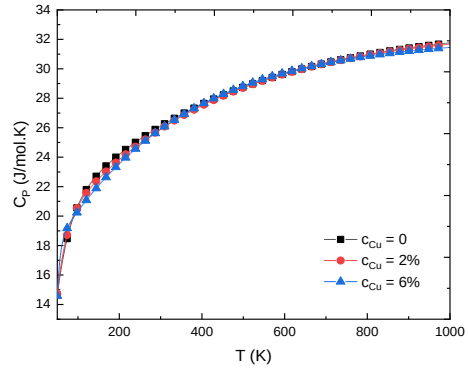

Figure 12. $C_P\left(T,c_{\mathrm{Cu}}\right)$ ***for AuCuLi at*** $c_{\mathrm{Li}}=0,6\%$

Table 4. Dependence of mean nearest neighbor distance $a(10^{-10}\mathrm{m})$ ***on temperature T and concentration of lithium atoms*** $c_{\mathrm{Li}}(\%)$ ***for AuCuLi at*** $c_{\mathrm{Cu}}=6\%$

***T*(K)**	***c*Li (%)**	**0**	**0.3**	**0.5**	**0.7**	**1**	**3**	**5**
50	$a(10^{-10}\mathrm{m})$	2.8069	2.8219	2.8292	2.8352	2.8431	2.8824	2.9162
100		2.8091	2.8242	2.8315	2.8376	2.8455	2.8852	2.9194
500		2.8270	2.8444	2.8529	2.8601	2.8698	2.9219	2.9689
700		2.8365	2.8599	2.8725	2.8839	2.8997	2.9941	3.0839
900		2.8464	2.8855	2.90870	2.9308	2.9630	3.16779	3.3684
1000		2.8516	2.9040	2.9363	2.9677	3.0138	3.31242	3.6067

Table 5. Dependence of mean nearest neighbor distance $a(10^{-10}\,\mathrm{m})$ ***on temperature T and concentration of copper atoms*** $c_{\mathrm{Cu}}(\%)$ ***for AuCuLi at*** $c_{\mathrm{Li}} = 0.6\%$

***T*(K**	$c_{\mathrm{Cu}}(\%)$	**0**	**0.5**	**1**	**2**	**3**	**4**	**5**	**6**
50	$a(10^{-10}\,\mathrm{m})$	2.853	2.851	2.849	2.846	2.842	2.839	2.835	2.83
100		2.855	2.853	2.851	2.848	2.845	2.841	2.838	2.83
300		2.864	2.862	2.861	2.857	2.854	2.851	2.847	2.84
500		2.875	2.874	2.872	2.869	2.866	2.863	2.859	2.85
700		2.897	2.895	2.894	2.891	2.887	2.884	2.881	2.87
900		2.940	2.938	2.937	2.933	2.930	2.926	2.923	2.91
1000		2.974	2.972	2.970	2.966	2.963	2.959	2.955	2.95

Table 6. Dependence of thermal expansion coefficient $\alpha_T\left(10^{-5}\,\mathrm{K}^{-1}\right)$ ***on temperature T and concentration of lithium atoms*** $c_{\mathrm{Li}}(\%)$ ***for AuCuLi at*** $c_{\mathrm{Cu}} = 6\%$

***T*(K)**	$c_{\mathrm{Li}}(\%)$	**0**	**0.3**	**0.5**	**0.7**	**1**	**3**	**5**
50	α_T $\left(10^{-5}\,\mathrm{K}^{-1}\right)$	0.9584	0.8557	0.6595	0.4505	0.3172	0.2992	0.1990
100		1.5615	0.9971	0.7418	0.6030	0.4299	0.1503	0.0665
500		2.0932	1.3615	1.0887	0.8977	0.7019	0.2884	0.1331
700		2.2440	1.4301	1.1456	0.9520	0.7553	0.2935	0.1649
900		2.4103	1.5012	1.1927	0.9855	0.7971	0.2964	0.1646
1000		2.6015	1.5306	1.2357	1.1025	0.8079	0.3972	0.2638

Table 7. Dependence of thermal expansion coefficient $\alpha_T\left(10^{-5}\,\mathrm{K}^{-1}\right)$ ***on temperature T and concentration of copper atoms*** $c_{\mathrm{Cu}}(\%)$ ***for AuCuLi at*** $c_{\mathrm{Li}} = 0.6\%$

***T*(K**	$c_{\mathrm{Cu}}(\%)$	**0**	**0.5**	**1**	**2**	**3**	**4**	**5**	**6**
50	α_T $\left(10^{-5}\,\mathrm{K}^{-1}\right)$	0.461	0.462	0.468	0.468	0.469	0.469	0.4693	0.469
100		0.674	0.678	0.679	0.679	0.770	0.770	0.7709	0.771
300		0.941	0.941	0.942	0.944	0.946	0.948	0.9498	0.950
500		0.986	0.987	0.989	0.991	0.993	0.995	0.9982	1.000
700		1.024	1.026	1.027	1.030	1.032	1.035	1.0378	1.040
900		1.062	1.064	1.065	1.068	1.071	1.074	1.0769	1.079
100		1.081	1.083	1.084	1.087	1.090	1.094	1.0970	1.100

Table 8. Dependence of heat capacity at constant pressure $C_P\left(\text{J/mol.K}\right)$ ***on temperature T and concentration of lithium atoms*** $c_{\text{Li}}(\%)$ ***for AuCuLi at*** $c_{\text{Cu}} = 6\%$

***T*(K)**	$c_{\text{Li}}(\%)$	**0**	**0.3**	**0.5**	**0.7**	**1**	**3**	**5**
50	C_P $\left(\text{J/ mol.K}\right)$	13.1718	13.2043	13.3981	13.9863	14.1863	14.3354	14.7759
100		21.3454	21.5393	21.6829	21.8319	22.0614	22.3479	22.7580
500		27.3840	27.3844	27.5073	27.6745	27.9715	30.3794	32.9576
700		28.7614	28.7879	29.0038	29.2891	29.7884	33.7619	37.9869
900		30.2616	30.3201	30.6562	31.0929	31.8494	37.7897	44.0722
1000		31.0810	31.1600	31.5710	32.1012	33.0156	40.1509	47.6776

Table 9. Dependence of heat capacity at constant pressure $C_P\left(\text{J/mol.K}\right)$ ***on temperature T and concentration of copper atoms*** $c_{\text{Cu}}(\%)$ ***for AuCuLi at*** $c_{\text{Li}} = 0.6\%$

***T*(K)**	$c_{\text{Cu}}(\%)$	**0**	**0.5**	**1**	**2**	**3**	**4**	**5**	**6**
50	C_P $\left(\text{J/ mol.K}\right)$	13.641	13.589	13.537	13.432	13.328	13.224	13.119	13.015
100		21.614	21.576	21.538	21.462	21.385	21.309	21.233	21.156
300		26.149	26.133	26.117	26.086	26.054	26.023	25.991	25.960
500		27.830	27.810	27.789	27.749	27.708	27.667	27.627	27.586
700		29.479	29.451	29.423	29.366	29.309	29.253	29.196	29.140
900		31.321	31.283	31.245	31.169	30.093	30.017	30.941	30.865
100		32.347	32.303	32.260	32.173	32.086	31.999	31.912	31.825

In the comparison of thermodynamic properties of alloys AuCuLi and AuCuSi we see that at the same temperature, pressure, the concentration of interstitial and substitutional atoms, the heat capacity at a constant pressure of AuCuLi is larger than that of AuCuSi and the thermal expansion coefficient of AuCuLi is smaller than that of AuCuSi. That is explained by the difference of the Mie-Lennard-Jones potential parameters between interstitial atoms Li and Si. The Mie-Lennard-Jones potential parameters are $n = 1.66$; $m = 3.39$; $D = 6800.502 \times 10^{-16}$ erg; $r_0 = 3.0077 \times 10^{-10}$ m [24-33] for Li and these parameters for Si are given in Table 1. The difference of potential parameters leads to the difference of the interstitial atom size and the interaction between the interstitial atom and main metal atoms. Therefore, at the same physical conditions, our calculated mean nearest neighbor distance between two atoms of AuCuLi is larger than that of AuCuSi. That leads to the difference of the heat capacity at constant pressure and the thermal expansion coefficient between AuSiLi and AuCuSi as above mentioned. For example at $P = 0$ and $T = 1000$ K, $AuCu_{6\%}Li_{5\%}$ has $a = 3.554 \times 10^{-10}$ m, $C_P = 47.74$ J/mol.K and $\alpha_T = 2.4 \times 10^{-5}$ K^{-1} while $AuCu_{6\%}Si_{5\%}$ has $a = 2.903 \times 10^{-10}$ m, $C_P = 32{,}12$ J/mol.K and $\alpha_T = 4.8 \times 10^{-5}$ K^{-1} [33].

3. Conclusions

We briefly present the thermodynamic theory of FCC ternary substitutional and interstitial alloy at zero pressure derived by the SMM and apply this theory to alloy AuCuLi. The thermodynamic properties of Au, AuCu and AuLi are specific cases for that of AuCuLi. Our calculated results of thermodynamic quantities for alloy AuCuLi predict and orient experimental results in the future. Our calculated results of the thermal expansion coefficient and the heat capacity at constant pressure in the interval of temperature from 100 to 700K for Au are in good agreement with experiments [33]. The calculated results of thermodynamic quantities for alloy AuCu are described in [25]. We compared the thermodynamic properties of alloys AuCuLi and AuCuSi in order to show the role of the size of the interstitial atom and the interaction between this atom and the main metal atom.

REFERENCES

[1] K. E. Mironov, 1967. *Interstitial alloy*. Plenum Press, New York.

[2] A. A. Smirnov, 1979. *Theory of interstitial alloys*, Nauka, Moscow (in Russian).

[3] A. G. Morachevskii and I. V. Sladkov, 1993. *Thermodynamic calculations in metallurgy*, Metallurgiya, Moscow (in Russian).

[4] V. A. Volkov, G. S. Masharov and S. I. Masharov, 2006. *Russian Physical Journal*, Vol. 49, No. 10, pp. 1084-1087.

[5] S. E. Andryushechkin, M. G. Karpman, 1999. *Metal Science and Heat Treatment*, Vol. 41, No. 2, pp. pp. 80-82.

[6] D. Batani; A. Balducci; D. Beretta; A. Bernardinello; T. Löwer; M. Koenig; A. Benuzzi; B. Faral, and T. Hall, 2000. Equation of state data for gold in the pressure range < 10 TPa, *Physical Review B*, Vol. 61, No. 14, pp. 9287-9294.

[7] K. Takemura and A. Dewaele, 2008. Isothermal equation of state for gold with a He-pressure medium. *Physical Review B*, 78, 104119, 13 pp.

[8] A. Dewaele, P. Loubeyre, F. Occelli, O. Marie and M. Mezouar, 2018. Toroidal diamond anvil cell for detailed measurements under extreme static pressures, *Nat. Commun*. Vol. 9, 2913, 9 pp.

[9] M. C. Daniel and D. Astruc, 2004. Gold nanoparticles: assembly, supramolecular chemistry, quantum-size-related properties and applications toward biology, catalysis and nanotechnology. *Chemical Review*, Vol. 104, No. 1, pp. 293-346.

[10] E. Yu. Tonkov and E. G. Ponuatovsky, 2005. Phase transformations of elements under high pressure, CRC Press, Boca, Raton, London, New York, Washington D.C.

[11] B. K. Godwal and R. Jeanloz, 1989. First-principles equation of state of gold, *Physical Review B*, Vol. 40, No. 11, pp. 7501-7507.

[12] M. Kumari and N. Dass, 1990. An equation of state applied to 50 solids: II. *Journal of Physics: Condensed Matter*, Vol. 2, pp. 7891-7895.

[13] G. W. Fernando, R. E. Watson, M. Weinert, Y. J. Wang and J. W. Davenport, 1990. Crystal structure of transition metals. *Physical Review B*, Vol. 41, pp. 11813-11818.

[14] H. L. Skriver, 1985. Crystal structure from one-electron theory. *Physical Review B*, Vol. 31, pp. 1909-1924.

[15] N.Sing, 1999. Structural phase transformation of Cu, Pd and Au using transition metal pair potential. *Physica B*, Vol. 269, pp. 211-220.

[16] P. Soderlind, 2002. Comment on "Theoretical prediction of phase transition in gold" by Ahuja. *Physical Review B*, Vol. 66, 176201 (1-2).

[17] J. C. Boettger, 2003. Theoretical extension of the gold pressure calibration standard beyond 3 Mbar. *Physical Review B*, Vol. 67, 174107 (1-7).

[18] H. Okamoto, D. J. Chakrabarti, D. E. Laughlin and T. B. Masalski, 1987. The Au-Cu (gold-copper) system. *Journal of Phase Equilibria*, Vol. 8, No. 5, 454.

[19] N. Q. Hoc, B. D. Tinh, L. D. Tuan and N. D. Hien, 2016. Elastic deformation of binary and ternary interstitial alloys with FCC structure and zero pressure: Dependence on temperature, concentration of substitution atoms and concentration of interstitial atoms. *Journal of Science of HNUE, Mathematical and Physical Sciences*, Vol 61, No. 7, pp. 47-57.

[20] N. Tang and V. V. Hung, 1989. Investigation of the thermodynamic properties of anharmonic crystals by the momentum method, I. General results for face-centered cubic crystals. *Physica Status Solidi (b)*, Vol. 149, 511-519.

[21] N. Tang and V. V. Hung, 1990. Investigation of the thermodynamic properties of anharmonic crystals by the momentum method, II. Comparison of calculations with experiments for inert gas crystals. *Physica Status Solidi (b)*, Vol. 161, pp. 165-171.

[22] N. Tang and V. V. Hung, 1990. Investigation of the thermodynamic properties of anharmonic crystals by the momentum method, III. Thermodynamic properties of the crystals at various pressures. *Physica Status Solidi (b)*, Vol. 162, pp. 371-377.

[23] N. Tang and V. V. Hung, 1990. Investigation of the thermodynamic properties of anharmonic crystals by the momentum method, IV. The limiting of absolute stability and the melting temperature of crystals. *Physica Status Solidi (b)*, Vol. 162, pp. 379-385.

[24] N. Q. Hoc, D. Q. Vinh, B. D. Tinh, T. T. C. Loan, N. L. Phuong, T. T. Hue, D. T. T. Thuy, 2015. Thermodynamic properties of binary interstitial alloys with a BCC structure: Dependence on temperature and concentration of interstitial atoms, *HNUE Journal of Science, Mathematical and Physical Sciences*, Vol. 60, No. 7, pp. 146.

[25] V. V. Hung, K. M. Jindo, P. D. Tam, S. R. Nishitani, 2001. Calculation of thermodynamic quantities of metals and alloys by the statistical moment method, *Journal of Phase Equilibria*, Vol. 22, No. 4, 400.

[26] N. Q. Hoc, P. T. M. Hanh and D. Q. Vinh, 2016. Thermodynamic property of binary interstitial alloy with FCC structure: Dependence on temperature and concentration of interstitial atoms. *Journal of Science of Hanoi University of Education No.2*, No. 46, pp. 39-50.

[27] V. V. Hung, 2009. *Statistical moment method in studying elastic and thermodynamic properties of crystals*, HNUE Publishing House.

[28] N. Q. Hoc, P. T. M. Hanh and L. H. Viet, 2016. Thermodynamic property of interstitial alloy AuSi with vacancy and FCC structure: Dependence on temperature, concentration of interstitial atoms and concentration of equilibrium vacancies. Proceedings of the 8th International Workshop on "Advanced Materials Science and Nanotechnology (IWAMSN-8)", 8-12th November 2016, Ha Long City, Vietnam. *Publishing House for Science and Technology*, pp. 293-301.

[29] N. Q. Hoc, P. T. M. Hanh and D. Q. Vinh, 2016. Thermodynamic property of binary interstitial alloy with FCC structure: Dependence on temperature and concentration of interstitial atoms. *HNUE Journal of Science,* Vol. 61, No. 8 pp. 39-50.

[30] N. Q. Hoc and D.Q.Vinh, 2017. Thermodynamic properties of binary interstitial alloy with FCC structure: Dependence on temperature and concentration of interstitial atoms, *Journal of Science of HNUE, Mathematical and Physical Sciences*, Vol. 62, No. 8, pp. 72-81.

[31] N. Q. Hoc, P. T. M. Hanh and L.H.Viet, 2017. Influence of vacancy on thermodynamic properties of interstitial alloy AuCuSi with FCC structure at zero pressure, Proceedings of the Conference "Transactions on Physics and Education" of Hanoi University of Education, No. 2, 15 December 2017, Xuan Hoa Town, Vinh Phuc Province. *Journal of Science of Hanoi University of Education No.*2, No. 50, pp. 118-129.

[32] M. N. Magomedov, 1987. On calculating the Debye temperature and the Gruneisen parameter. *Zhurnal Fizicheskoi Khimii,* Vol. 61, No. 4, pp. 1003-1009.

[33] *American Institute of Physics Handbook*, 1963, New York.